

Raman scattering and photoluminescence from Si nanoparticles in annealed SiO_x thin films

D. Nesheva,^{a)} C. Raptis,^{b)} and A. Perakis

Department of Physics, National Technical University of Athens, GR-15780 Athens, Greece

I. Bineva, Z. Aneva, Z. Levi, and S. Alexandrova

Institute of Solid State Physics, Bulgarian Academy of Sciences, 1784 Sofia, Bulgaria

H. Hofmeister

Max Planck Institute of Microstructure Physics, D-06120 Halle, Germany

(Received 20 November 2001; accepted for publication 11 July 2002)

Silicon-rich silicon oxide thin films have been prepared by thermal evaporation of silicon monoxide in vacuum. The SiO_x film composition ($1.1 \leq x \leq 1.7$) has been controlled by varying the deposition rate and residual pressure in the chamber. Long time stability of all films has been ensured by a postdeposition annealing at 523 K for 30 min in Ar atmosphere. Some films were further annealed at 973 K and some others at 1303 K. Raman scattering measurements have implied the formation of amorphous silicon nanoparticles in films annealed at 973 K and Si nanocrystals in films annealed at 1303 K. The latter conclusion is strongly supported by high resolution electron microscopy studies which show a high density of Si nanocrystals in these films. Photoluminescence has been observed from both amorphous and crystalline nanoparticles and interpreted in terms of band-to-band recombination in the nanoparticles having average size greater than 2.5 nm and carrier recombination through defect states in smaller nanoparticles. © 2002 American Institute of Physics. [DOI: 10.1063/1.1504176]

I. INTRODUCTION

Although crystalline silicon is a key material in the microelectronic industry, its use in optoelectronic applications is hindered because, as an indirect gap semiconductor, its light emission in the visible is inefficient. The observation of strong visible photoluminescence from porous silicon at room temperature¹ stimulated substantial activity in the field of preparation of structures comprising silicon nanowires and nanoparticles as well as exploration of their structural and optoelectronic properties. Later, intense visible photoluminescence has been reported from nanocrystalline silicon films²⁻⁴ and SiO₂ thin films containing crystalline⁵⁻¹⁵ or amorphous^{10,13,16-19} silicon nanoparticles. Often, this luminescence has been attributed to radiative recombination of carriers confined in Si nanoparticles and its color can be suitably modified by changing the nanoparticle size.

Silicon nanoparticles in Si-rich silicon oxide films are generally produced by high-temperature annealing in an inert atmosphere. The process is compatible with integrated circuit technology¹ and, moreover, SiO₂ is a robust host that provides good passivation for the Si nanoparticles. In this approach the average nanoparticle size (and the emission properties) can be properly tuned either by varying the annealing temperature or by changing the excess silicon content in the deposited films. Several techniques have been employed to make Si-rich SiO_x thin films ($x < 2$), which include high-dose Si ion implantation into SiO₂ films,^{5,6} deposition of

SiO_x films by cosputtering,^{8,17,20} and electron beam coevaporation²¹ of Si and silicon monoxide (SiO), plasma enhanced chemical vapor deposition,^{7,9-11} laser ablation of Si in ambient oxygen,¹² and thermal vacuum or reactive evaporation of SiO.^{14,15,18}

The ability to control the size and structure of nanoparticles would allow the fabrication of structures with desired electrical and optoelectronic properties for device applications. Raman scattering provides a fast and nondestructive method to determine whether silicon particles are amorphous or crystalline. Moreover, information about nanocrystallite size can be obtained from the shape and peak position of the first order Raman scattering band.²²⁻²⁶ In crystalline materials this band has a Lorentzian line shape with an intrinsic linewidth of about 3 cm^{-1} at room temperature. The “finite size effects,” which destroy the full translation symmetry of the material, result in a low-frequency asymmetric broadening and redshift of the Raman band. Thus, from the details of the Raman line shape the nanoparticle size could be determined.^{22,23,26} However, when applying this approach one should remember that other effects, such as structural damage, alloying, etc., also produce similar changes.²⁵ Besides, tensile and compressive stresses affect the Raman line by a red- and blueshift, respectively.

The evaporation of silicon monoxide is a rather straightforward method for preparation of SiO_x thin films, but up to now little work has been published on this subject. In this article, SiO_x thin films with oxygen content x , varying between 1.1 and 1.7, have been produced by thermal evaporation of SiO in vacuum. Amorphous and crystalline silicon nanoparticles have been grown upon annealing the films at 973 and 1303 K, respectively; the presence of Si nanocryst-

^{a)}On leave from: Institute of Solid State Physics, Bulgarian Academy of Sciences, 1784 Sofia, Bulgaria.

^{b)}Author to whom correspondence should be addressed; electronic mail: craptis@central.ntua.gr

TABLE I. Deposition rate V_d of α -SiO_x thin films prepared by thermal evaporation of silicon monoxide and the corresponding oxygen content x values derived from Rutherford backscattering measurements.

V_d (nm/s)	High residual pressure (1×10^{-3} Pa)			Low residual pressure (2×10^{-4} Pa)			
	0.2	3.0	6.0	0.2	1.0	3.0	6.0
x	1.7	1.3	1.15	1.6	1.4	1.2	1.1

tals in the latter films has been detected by high resolution electron microscopy (HREM). Raman scattering measurements have been carried out in both sets of films, providing further evidence for the formation of Si nanocrystals in films annealed at 1303 K. Photoluminescence in the visible and near infrared region has been observed from films containing amorphous or crystalline particles.

II. EXPERIMENT

Films of SiO_x were prepared by evaporation of SiO from a tantalum crucible (heated to 1550–1670 K, depending on the deposition rate) equipped with a molybdenum cylindrical screen which restricted spreading of the SiO vapor inside the vacuum chamber. Crystalline silicon (Wacker, *p*-type) substrates were used. Both the molybdenum screen and the substrate were at room temperature, but some increase of their temperature might have taken place as a result of radiative heating by the crucible. The native oxide of the *c*-Si substrates was not removed. The films were deposited under two different residual pressures of 1×10^{-3} Pa (high pressure) and 2×10^{-4} Pa (low pressure). The film thickness (between 0.2 and 2 μ m) and deposition rate (0.2, 1.0, 3.0, and 6.0 nm/s) were controlled by a preliminarily calibrated quartz microbalance system MIKI FFV. In order to ensure long time stability of SiO_x films, that is, independent of humidity conditions, all films prepared were annealed at 523 K for 30 min in argon immediately after taking them out of the vacuum system.²⁷ Afterward the following annealing procedures were carried out on different groups of samples: (i) at 973 K for 60 min in argon or air, (ii) at 1273 K for 60 min in argon, and (iii) at 1303 K for 60 min in nitrogen. The film composition has been investigated by Rutherford backscattering²⁷ and the resulting oxygen contents determined in this way are shown in Table I.

HREM measurements were performed in SiO_x films deposited on Si substrates and annealed at 973 and 1273 K by means of a JEM 4000 EX electron microscope operating at 400 kV. Electron micrographs were recorded at 500 000 times magnification using optimum contrast conditions (near Scherzer defocus). Stokes Raman spectra in a pseudobackscattering geometry (with occasional scans of the anti-Stokes region being also carried out) and photoluminescence from all kinds of SiO_x films were measured using a system of a SPEX double monochromator and cooled photomultiplier in connection with photon counting equipment. The spectral slit width was set at 2.5 cm⁻¹. The 488 nm line of an Ar⁺ laser was used for the excitation focused on the sample surface by a cylindrical lens in order to avoid deterioration of the films. The laser beam power density used was ~ 4 W/mm² for the

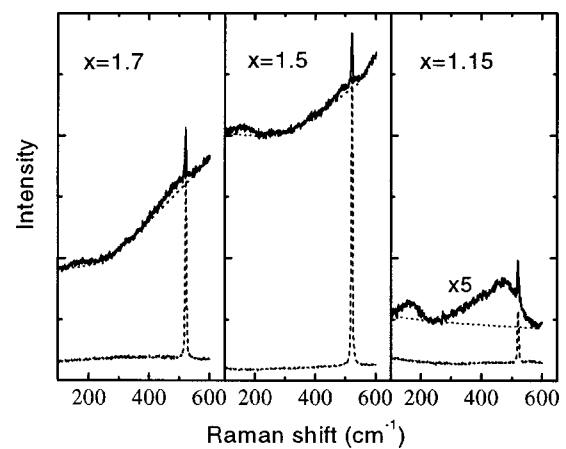


FIG. 1. Raman spectra of SiO_x films having oxygen content $x = 1.15$, 1.5, and 1.70 excited by the 488 nm Ar⁺ laser line. The films were annealed at 523 K for 30 min in argon atmosphere (dashed spectra) and then at 973 K for 60 min, again in argon atmosphere (solid spectra). All spectra correspond to the same scale.

Raman scattering measurements and 1 or 2 W/mm² for the photoluminescence ones. The thickness of the SiO_x films for the Raman measurements was 1 μ m but, in order to avoid light interference, samples having thickness of 0.2 μ m were used for the luminescence measurements. All spectra were measured at 293 K in air.

III. RESULTS AND DISCUSSION

A. Raman scattering

1. Amorphous silicon nanoparticles

Raman spectra of SiO_x films ($x = 1.15$, 1.5, and 1.70) deposited at high residual pressure and annealed at 523 K show (Fig. 1, dashed spectra) only one strong sharp peak at 520 cm⁻¹ having full width at half maximum (FWHM) of 4.5 cm⁻¹. We have determined the same parameters for the transverse optical (TO) phonon band of bare silicon substrate, which indicates that the intense band in samples annealed at 523 K originates from the crystalline silicon substrate; the lack of other features in the spectrum of these films implies the absence of other phases, such as amorphous Si. This is in agreement with the results of other authors for evaporated and sputtered SiO_x films with $x \geq 1$ ^{18,28} who have suggested Si phase separation at temperatures $T > 673$ K.

Cross-section electron micrographs of the films annealed at 973 K indicated an absence of any crystalline phase. However, significant changes are seen in their Raman scattering spectra (Fig. 1, solid spectra). A strong photoluminescence background is observed in the samples having high oxygen content $x \geq 1.5$. Such a background is not seen in the spectrum of the sample with $x = 1.15$. Moreover, the intensity of the 520 cm⁻¹ band is significantly reduced after annealing at 973 K and two new bands at ~ 160 and ~ 480 cm⁻¹ appear. They are well resolved in the film with $x = 1.15$, but also exist in the other spectra. It is known^{18,23,29} that amorphous silicon generally exhibits strong bands at ~ 150 and ~ 480 cm⁻¹. Hence, the appearance of similar bands in the SiO_x films annealed at 973 K indicates that, upon annealing, some Si phase separation occurs, which results in the formation of

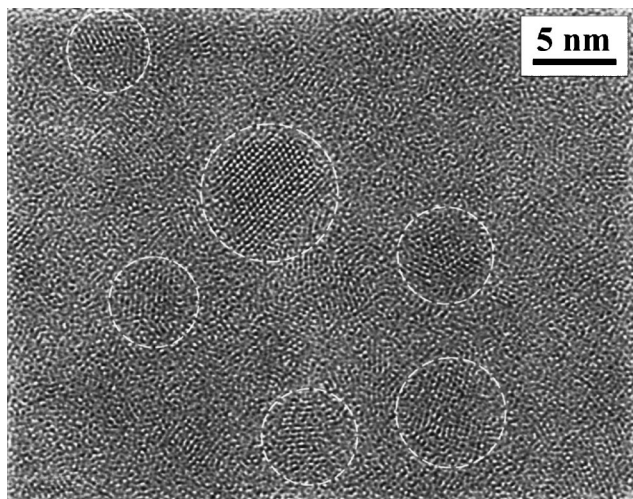


FIG. 2. Cross-section micrograph of a SiO_x film with $x=1.3$ annealed at 1273 K for 60 min in argon atmosphere. Si nanocrystals can be seen uniformly distributed in the matrix. The shape of some nanocrystals is close to spherical while others are anisotropically grown.

small-size amorphous silicon regions in the SiO_x matrix. The observed decrease of the 520 cm^{-1} band intensity supports this suggestion since absorption of $a\text{-Si}$ in the blue wavelength region is significantly higher than that of SiO_x ($x > 1$). In addition, infrared absorption measurements²⁷ have shown an increase in the oxygen content of the SiO_x matrix after annealing at 973 K. What is the size of the amorphous Si regions? As mentioned above, Si is an indirect band gap semiconductor and in bulk form it does not show photoluminescence; radiative recombination may be observed only in silicon particles in which at least one of its dimensions is less than the free exciton radius¹ (Bohr radius ~ 5 nm) of bulk Si. The strong photoluminescence background in the Raman spectra of the films with oxygen content $x \geq 1.5$ implies that, if this luminescence has a quantum confinement origin, the size of the amorphous silicon nanoparticles in these samples should be a few nanometers.

2. Silicon nanocrystals

The infrared absorption measurements carried out on the SiO_x films annealed at 1303 K have shown²⁷ a complete phase separation with the silicon nanoparticles grown within a SiO_2 matrix. A cross-section micrograph of such a Si– SiO_2 film (with an initial oxygen content of $x=1.3$) annealed at 1273 K for 60 min is shown in Fig. 2 in which a quite high density of Si nanocrystals can be seen; the shape of some nanocrystals is close to spherical, while others are anisotropically grown with an aspect ratio of ~ 2 . They are uniformly distributed in the matrix and their size ranges between about 2 and 8 nm, with a mean diameter of ~ 4.3 nm. On the other hand an average nanocrystallite size of 2.6 nm has been obtained for the average nanocrystallite size for the film with $x=1.5$. So, in agreement with other authors,^{8,11,14,15} we have observed a qualitative increase of the average nanoparticle size with decreasing x and it can be expected that the average size of nanocrystals for films with $x=1.6, 1.7$ is below 2.5 nm.

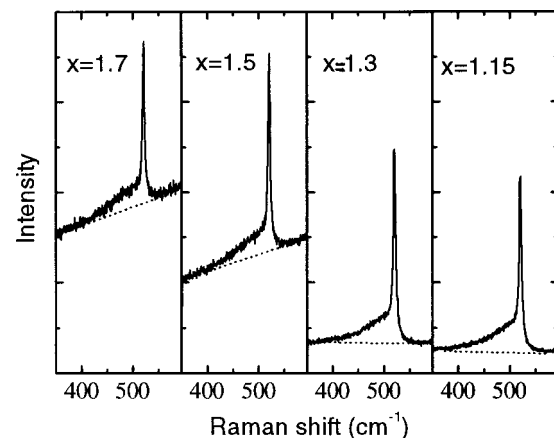


FIG. 3. Raman spectra of SiO_x films having oxygen content $x=1.15, 1.3, 1.5,$ and 1.7 annealed at 523 K for 30 min in argon atmosphere and then at 1303 K for 60 min in nitrogen. All spectra correspond to the same scale.

Raman spectra of four SiO_x films with different oxygen content deposited on crystalline Si substrates and annealed at 1303 K for 60 min are shown in Fig. 3. The spectra exhibit, essentially, two components—a sharp peak at 520 cm^{-1} and a low-energy tail which does not evolve into a clearly distinguishable peak in any sample. As in the films annealed at 973 K, the sharp component can be assigned to the substrate. We suggest that the tail represents mostly scattering from silicon nanocrystals grown upon annealing and this is supported by a similar low-energy tail observed in other Si nanocrystal Raman studies.^{23–25} In those studies,^{23–25} the peak of the Raman band is not significantly shifted (relative to the Si single crystal band), but its low-energy tail is highly asymmetric extending down to 450 cm^{-1} in a fashion similar to that of the tail of our Raman spectra (Fig. 3). However, some small part of the scattering in the low-frequency tail of our spectra (Fig. 3) may be due to $a\text{-Si}$ which has a Raman peak^{18,23,29} at $\sim 480\text{ cm}^{-1}$ extending asymmetrically down to $250\text{--}300\text{ cm}^{-1}$. We do not observe any scattering below 400 cm^{-1} and this implies that most of the scattering in the low-energy tail of our spectra is due to Si nanocrystals. This conclusion is also supported by our HREM results (Fig. 2) which show quite a high density of Si nanocrystals in the films annealed at 1273 K. The existence of a significant concentration of $a\text{-Si}$ nanoparticles (not seen by transmission electron microscopy) in these films does not seem plausible because of their rather high oxygen content ($1.1 < x < 1.7$).

Raman spectra have been used^{8,24,30} in the past for the evaluation of the average size of Si and Ge nanocrystals. This can be achieved either by fitting the experimental curve with some expression, which takes into account the finite size effects,^{24,30} or, roughly, by using the theoretically predicted relations^{22,24–26} of the band position and asymmetry with crystallite size. In both approaches the accurate determination of the nanocrystallite band is very important, especially for films grown on $c\text{-Si}$ substrates in the Raman spectra of which the 520 cm^{-1} band also appears. In nanocrystalline Si films the scattered light from the film is quite intense, but scattering from the substrate is significantly reduced by the absorption in the film. This implies that the

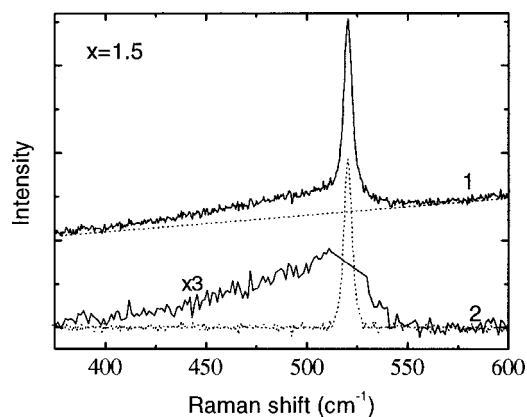


FIG. 4. Recorded Raman spectrum of a SiO_x film with $x=1.5$ (spectrum 1) and spectrum obtained after subtraction of a baseline (including luminescence and noise background) and a Lorentzian band peaked at 520 cm^{-1} (corresponding to the Raman band of c -Si substrate); the resulting spectrum corresponds to scattering from Si nanocrystals. The dotted lines represent a baseline including the luminescence background and noise and the Lorentzian band at 520 cm^{-1} with FWHM of 4.5 cm^{-1} (components subtracted from the recorded spectrum).

shape and position of the band originating from the nanocrystals²³ are not expected to be distorted by scattering from the substrate. However, in Si-SiO₂ films the filling factor is relatively low ($<10\%$)¹⁴ and the intensity of light scattered from Si nanocrystals is quite low, while the Raman line due to the c -Si substrate is rather strong.

One can see from Fig. 3 that the sharp band in all spectra peaks at 520 cm^{-1} and has FWHM of 4.5 cm^{-1} . Obviously, scattering from the Si nanocrystals is rather weak and does not affect appreciably the shape and position of the substrate band. In an attempt to resolve the nanocrystallite band, we have subtracted from the measured spectrum of each film (see Fig. 4): (i) a baseline including the luminescence background and noise and (ii) a Lorentzian band having the above peak position and FWHM. First, the Lorentzian amplitude was taken to be equal to that of the 520 cm^{-1} band in the measured spectra. After this subtraction, the resulting broadband (spectrum 2 of Fig. 4) peaks at about 510 cm^{-1} , showing an anticipated shift (in comparison to the peak position of the previously observed Si nanocrystals Raman band²³⁻²⁵) because in subtracting the sharp Lorentzian band, inevitably we have also subtracted scattering due to nanocrystals whose band also peaks around 520 cm^{-1} . This is reflected by the variable position and shape of the band after subtraction which have been found to depend on the amplitude used for the sharp Lorentzian band.

Since the precise intensity level of scattered light from the c -Si substrate cannot be determined, we conclude that it is not possible to determine correctly the Si nanocrystallite size from Raman scattering spectra of Si-SiO₂ thin films having a low filling factor.

B. Photoluminescence

Figure 5 shows photoluminescence (PL) spectra of SiO_x films with different oxygen content annealed at 973 K for 60 min [upper spectra in (a), (b), and (c)] and at 1303 K for 60 min [lower spectra in (a), (b), (c), and (d)]. All samples have

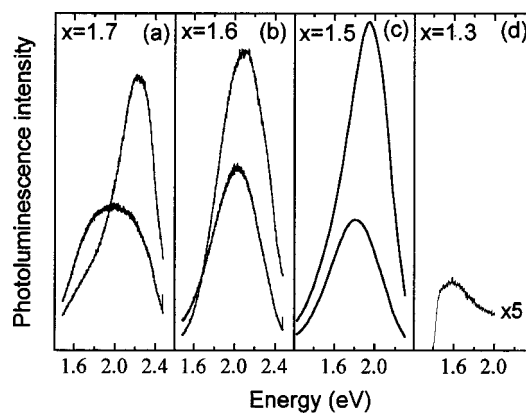


FIG. 5. Photoluminescence spectra of SiO_x films with different oxygen content annealed at 973 K for 60 min in argon [(a), (b), and (c), upper spectra] or 1303 K for 60 min in nitrogen [(a), (b), (c), and (d), lower spectra]. All samples have the same thickness of $0.2\text{ }\mu\text{m}$. All spectra were excited by the 488 nm Ar^+ laser line and correspond to the same scale.

the same thickness of $0.2\text{ }\mu\text{m}$. In the films with low oxygen content ($x \leq 1.3$), photoluminescence is rather weak after annealing at 1303 K and absent in the samples annealed at 973 K. In the films with high oxygen content ($x=1.6, 1.7$), the luminescence bands are disposed in the red-green spectral range and their peak energy is much higher than the optical band gap of bulk silicon (1.11 eV). Generally, for both annealing temperatures the emission bandshifts to the red with decreasing oxygen content, but for the same initial composition, the photoluminescence band of amorphous silicon nanoparticles is blueshifted compared to that of nanocrystals. The intensity of emitted light shows a nonmonotonous change with composition for each annealing temperature. A similar observation has also been reported by other authors.^{8,13,15} This nonmonotonous change can be attributed to competing effects caused by carrier confinement and excess of silicon atoms in SiO_x films. Furthermore, the confinement effect becomes weaker with decreasing oxygen content and increasing nanocrystallite size which, because of the indirect band gap of c -Si, leads to an intensity decrease. On the other hand, the total amount of Si crystallites increases when x decreases.

Photoluminescence from nanosized crystalline silicon has been generally attributed to band-to-band radiative recombination of electron-hole pairs confined within such nanoparticles (the quantum confinement model^{1,5,31,32}). It is presumed that for such a radiative process, the excitation energy should be higher than the optical band gap energy of Si nanoparticles. Diverse theoretical values for the optical band gap energy of Si nanocrystals have been obtained by various models, such as the effective-mass model, the tight-binding model, the density-functional model, etc. (see Ref. 31 and references therein). Some models³² predict relatively high values for the optical band gap of nanocrystals (ranging from 1.6 and 2.3 eV for nanocrystal average size between 5.0 and 2.5 nm, respectively), while others³¹ produce lower values, closer to the experimental ones; for example, for an average nanocrystallite size of 1.5 nm, the optical band gap does not exceed the value of 2.5 eV. Since the excitation energy used in our luminescence experiments is 2.54 eV (488 nm Ar^+

laser line), this energy is adequate (high enough) for band-to-band luminescence excitation of our films. Of course, a better picture of the band structure of the Si nanocrystals of this work could be obtained using a variety of excitation energies, including also much higher ones than their estimated optical gap energies, and this is one of our tasks for the near future. It must be pointed out that there are diverse results concerning the position of photoluminescence of Si nanocrystals with exciting energy. Some authors³³ have reported a blueshift of PL position with exciting energy, while in other reports,^{34–36} excitation with either the 325 nm line from a He–Cd laser or the 488 nm line of an Ar⁺ laser produced similar PL; in the first of these reports,³⁴ the nanocrystallite sizes vary between 2 and 4.7 nm, which is similar to ours.

In the films with $x=1.3$ (average nanocrystallite size of ~ 4.3 nm) and $x=1.5$, we have observed a PL band peaking at 1.6 and 1.8 eV (Fig. 5), respectively, and these values are close to the expected position for band-to-band recombination. However, in the films with $x=1.6$ and 1.7, in which average nanocrystallite sizes less than 2.5 nm are expected, the observed PL peak energy of ~ 2 eV (Fig. 5) is below the predicted values of >2.3 eV.³¹ Other groups^{11,37,38} have also reported that, when the Si crystallite size drops below 3 nm, the photoluminescence peak does not exceed the value of 2.1 eV. In a recent study on porous Si,³⁹ PL from Si nanocrystals smaller than 3 nm has been attributed to radiative recombination which involves an electron trapped by Si=O double bonds at the interface (producing localized states in the band) and a free hole. The PL emission energy still increases, but not as fast as predicted by the quantum confinement model. For sizes below 2 nm, recombination via trapped excitons has been suggested and no further PL energy increase is expected. It has been assumed³⁹ that the existence of large stress at the Si–SiO₂ interface creates dangling bonds at the Si nanocrystal surface and Si=O double bonds at the interface appear to passivate partly these dangling bonds. Based on this model, carrier recombination through defect states rather than band-to-band recombination may be assumed in SiO_x films with high oxygen content ($x=1.6, 1.7$) and expected nanocrystallite size <2.5 nm.

Now we turn our attention to the PL from the films annealed at 973 K, which contain amorphous silicon nanoparticles (Fig. 1). Such PL has been observed only in films with high oxygen content ($x \geq 1.5$) and the PL band peaks between 2 and 2.2 eV. It is blueshifted and more intense compared to the band from nanocrystals grown in the film with the same initial composition but annealed at 1303 K (Fig. 5). Intense PL has already been observed from SiO_x films containing amorphous silicon nanoparticles^{10,13,17–19} and porous *a*-Si:H.⁴⁰ The PL intensity increases and its peak energy blueshifts with decreasing nanoparticle size. It is interesting that in some publications^{10,19} a quite strong blueshift (from ~ 1.6 eV, the band gap of bulk *a*-Si, to ~ 2.0 eV) has been reported while in another one⁷ it is smaller (from ~ 1.6 to ~ 1.8 eV). Most authors have explained these results in terms of the quantum confinement model,^{10,13,17–19} although it has been argued⁴¹ that quantum confinement of holes in *a*-Si should be absent and that of electrons is marginal for sizes

larger than 1–2 nm because of their low mobilities. The high PL intensity has also been interpreted in terms of spatial carrier confinement.^{40,41} Since the average size of amorphous nanoparticles is less than the capture radius for nonradiative recombination, the quantum efficiency is expected to increase substantially. The spatial carrier confinement also predicts a blueshift of the PL band with decreasing size.⁴¹ When the nanoparticle size decreases, the separation between localized tail states (whose recombination produces luminescence) increases. This causes thermalization of electrons down to the lowest lying tail states and radiative recombination occurs between higher states in the conduction band tail and low lying holes in the valence band tail. Such a mechanism could be responsible for the red PL, but it cannot explain PL in the yellow–green spectral range. Thus, we reckon that PL from the SiO_x ($x \geq 1.5$) films annealed at 973 K may be due to radiative recombination of carriers which are quantum confined in very small amorphous Si nanoparticles. Indeed, for the same composition of SiO_x films, nanocrystallite size increases with temperature^{4,10,11,13} and, hence, the size of amorphous silicon nanoparticles in films annealed at 973 K should be smaller than that of nanocrystals (2.6 nm for $x=1.5$) grown upon annealing at 1303 K. The assumption for carrier quantum confinement in amorphous nanoparticles, which are smaller than crystalline ones, may explain both the blueshift of the PL bands from the films annealed at 973 K (Fig. 5) and the higher PL intensity from amorphous silicon nanoparticles. (We recall that, upon annealing at 973 K, the phase separation is not completed, while at 1303 K it is completed; thus, one can expect that the total volume of the *a*-Si phase formed after annealing at 973 K should be slightly smaller than that of the nc-Si phase). The lack of PL in films with $x=1.3$ annealed at 973 K and its appearance upon annealing at 1303 K favors the idea for marginal carrier quantum confinement in *a*-Si for sizes larger than 2 nm.

IV. CONCLUSIONS

Thermal evaporation of silicon monoxide in vacuum has been used for deposition of SiO_x thin films with oxygen content varying between 1.1 and 1.7. Long time stability of the films has been achieved by a postdeposition annealing at 523 K for 30 min. There is strong evidence that amorphous and crystalline silicon nanoparticles of various sizes have been formed upon annealing at 973 and 1303 K, respectively. It has been established that, due to the low volume fraction of the silicon nanocrystals in the films, both shape and position of the 1TO band of their Raman spectra are strongly affected by scattering from the substrate and this effect is a serious drawback in determining their size. Light emission has been observed from both amorphous and crystalline nanoparticles whose peak position redshifts from yellow to the near infrared with increasing nanoparticle size. This PL has been interpreted in terms of band-to-band recombination in the nanoparticles having average size greater than 2.5 nm and carrier recombination through defect states in smaller nanoparticles.

ACKNOWLEDGMENTS

D.N. wishes to thank the National Technical University of Athens for support of the Raman scattering and photoluminescence measurements. The authors are very grateful to Dr. J.-K. Pivin who performed Rutherford backscattering measurements.

- ¹L. T. Canham, *Appl. Phys. Lett.* **57**, 1046 (1990).
- ²F. Huisken, H. Hofmeister, B. Kohn, M. A. Laguna, and V. Paillard, *Appl. Surf. Sci.* **154–155**, 305 (2000).
- ³Z. H. Lu, D. J. Lockwood, and J.-M. Baribeau, *Nature (London)* **378**, 258 (1995).
- ⁴V. Vinciguerra, G. Franzo, F. Priolo, F. Iacona, and C. Spinella, *J. Appl. Phys.* **87**, 8165 (2000).
- ⁵F. Koch and V. Petrova-Koch, *J. Non-Cryst. Solids* **198–200**, 840 (1996).
- ⁶M. L. Brongersma, A. Polman, K. S. Min, E. Boer, T. Tambo, and H. A. Atwater, *Appl. Phys. Lett.* **72**, 2577 (1998).
- ⁷F. N. Timofeev, A. Aydinli, R. Ellialtioglu, K. Turkoglu, M. Gure, V. N. Mikhailov, and O. A. Lavrova, *Solid State Commun.* **95**, 443 (1995).
- ⁸I. Balberg (private communication).
- ⁹S. Veprek, *Thin Solid Films* **297**, 145 (1997).
- ¹⁰Zh. Ma, X. Liao, J. He, W. Cheng, G. Yue, Y. Wang, and G. Kong, *J. Appl. Phys.* **83**, 7934 (1998).
- ¹¹F. Iacona, G. Franzo, and C. Spinella, *J. Appl. Phys.* **87**, 1295 (2000).
- ¹²K. Murakami, T. Suzuki, T. Makimura, and M. Tamura, *Appl. Phys. A: Mater. Sci. Process.* **69**, S13 (1999).
- ¹³Y. Wakayama, T. Tagami, T. Inokuma, S. Hasegawa, and Sh. Tanaka, *Res. Dev. Cryst. Growth* **1**, 83 (1999).
- ¹⁴U. Kahler and H. Hofmeister, *Appl. Phys. Lett.* **75**, 641 (1999).
- ¹⁵U. Kahler and H. Hofmeister, *Opt. Mater.* **17**, 83 (2001).
- ¹⁶M. Zaharias, H. Freistdt, F. Stolze, T. P. Drusedau, M. Rosenbauer, and M. Stutzmann, *J. Non-Cryst. Solids* **164–166**, 1089 (1993).
- ¹⁷S. Hayashi and K. Yamamoto, *J. Lumin.* **70**, 352 (1996).
- ¹⁸H. Rinnert, M. Vergnat, G. Marchal, and A. Burneau, *J. Lumin.* **80**, 445 (1999).
- ¹⁹H. Rinnert, M. Vergnat, and G. Marchal, *Mater. Sci. Eng., B* **69–70**, 484 (2000).
- ²⁰Li. You, C. L. Heng, S. Y. Ma, Z. C. Ma, W. H. Zong, Zh. Wu, and G. G. Qin, *J. Cryst. Growth* **212**, 109 (2000).
- ²¹S. Zhang, W. Zhang, and J. Yuan, *Thin Solid Films* **326**, 92 (1998).
- ²²H. Richter, Z. P. Wang, and L. Ley, *Solid State Commun.* **39**, 625 (1981).
- ²³Z. Iqbal and S. Veprek, *J. Phys. C* **15**, 377 (1982).
- ²⁴J. Gonzales-Hernandez, G. H. Azarbajegani, R. Tsu, and F. H. Pollak, *Appl. Phys. Lett.* **47**, 1350 (1985).
- ²⁵I. H. Campbell and P. M. Fauchet, *Solid State Commun.* **52**, 739 (1986).
- ²⁶J. Zi, H. Buscher, C. Falter, W. Ludwig, K. Zhang, and X. Xie, *Appl. Phys. Lett.* **69**, 200 (1996).
- ²⁷D. Nesheva, Z. Levi, Z. Aneva, I. Bineva, Tz. Merdzhanova, and J. C. Pivin, *Vacuum* (in press).
- ²⁸G. Hollinger, Y. Jugnet, and T. M. Duc, *Solid State Commun.* **22**, 277 (1977).
- ²⁹J. E. Smith, Jr., M. H. Brodsky, B. L. Crowder, M. I. Nathan, and A. Pinczuk, *Phys. Rev. Lett.* **26**, 642 (1971).
- ³⁰D. R. dos Santos and I. L. Torriany, *Solid State Commun.* **85**, 307 (1993).
- ³¹J.-B. Xia and K. W. Cheah, *Phys. Rev. B* **59**, 14876 (1999).
- ³²C. Delerue, G. Allan, and M. Lannoo, *Phys. Rev. B* **48**, 11024 (1993).
- ³³G. Belomoin, J. Therrien, and M. Nayfeh, *Appl. Phys. Lett.* **77**, 779 (2000).
- ³⁴L. D. Dinh, L. L. Chase, M. Balooch, W. J. Siekhaus, and F. Wooten, *Phys. Rev. B* **54**, 5029 (1996).
- ³⁵S.-T. Chou, J.-H. Tsai, and B.-C. Shen, *J. Appl. Phys.* **83**, 5394 (1998).
- ³⁶D. Nesheva, C. Raptis, and Z. Levi, *Phys. Rev. B* **58**, 7913 (1998).
- ³⁷S. Schuppler *et al.*, *Phys. Rev. B* **52**, 4910 (1995).
- ³⁸J. von Behren, T. van Buuren, M. Zacharias, E. H. Chimowitz, and P. M. Fauchet, *Solid State Commun.* **105**, 317 (1998).
- ³⁹M. V. Wolkin, J. Jorne, P. M. Fauchet, G. Allan, and C. Delerue, *Phys. Rev. Lett.* **82**, 197 (1999).
- ⁴⁰R. B. Wehrspohn, J.-N. Chazalviel, F. Ozanam, and I. Solomon, *Phys. Rev. Lett.* **77**, 1885 (1996).
- ⁴¹S. A. Koehler, *Philos. Mag. B* **77**, 27 (1998).